Vol 3 (2) (2022)

Measurement, Control, and Automation

Website: https:// mca-journal.org

ISSN 1859-0551

A new neural iterative learning control approach for position tracking control of robotic manipulators: Theory, simulation, and experiment

Dang Xuan Ba[1]* and Trong-Tai Nguyen[2]

[1]*Department of Automatic Control, Ho Chi Minh City University of Technology and Education (HCMUTE)*
[2]*Department of Automatic Control, Ho Chi Minh City University of Technology (HCMUT)*
Corresponding author E-mail: badx@hcmute.edu.vn

Abstract

This paper presents a new effective iterative learning control method for repetitive motion-tracking control problems of robotic manipulators. The controller is comprised of two control loops. In the inner loop, a simple proportional-derivative signal is adopted to stabilize the closed-loop system that facilitates design of the outer loop. Tracking control mission is mainly achieved by a novel iterative control signal designed in the outer loop. The effectiveness of the proposed control method is resulted in from a new iterative design where the iterative signal is flexibly structured from both the current and previous information on the iterative axis. To this end, a neural network is developed to estimate the iterative disturbances using information synthesized from the past and present iterations. A proper inherent function is then employed to connect the iterative-based and time-based control signals. Stability of the overall system is analyzed using absolution regression series criteria. The effectiveness and feasibility of the proposed controller are intensively discussed based on the comparative simulation results and real-time experiments obtained from a 6 degree-of-freedom robot.

***Keywords**: Motion Control, Iterative Learning Control, Neural Network, Robotic Manipulator, Simulation*

Symbols

Symbols	Units	Description
$c(\cdot)$		Function of variable $\cdot$
$\mathbf{q}$	rad	Vector of joint position
$\mathbf{M}(\mathbf{q})$	kg	Inertia-mass matrix
$\mathbf{C}(\mathbf{q},\dot{\mathbf{q}})\dot{\mathbf{q}}$	N.m	Coriolis/Centripetal effect in robotic models
$\mathbf{g}(\mathbf{q})$	N.m	Gravitational torque in robotic models
$\mathbf{f}(\dot{\mathbf{q}})$	N.m	Frictional torque in robotic models
$\boldsymbol{\tau}_d$	N.m	External disturbances in robotic models
$\boldsymbol{\tau}$	N.m	Joint torque or control signal in robotic models

Abbreviations

DOF	Degree of Freedom
PID	Proportional Integral Derivative
ILC	Iterative Learning Control
TNN	Time-based Neural Network
TNNIC	Time-based Neural Network Iterative Control

Tóm tắt

Bài báo này trình bày một phương pháp điều khiển học lặp mới để giải quyết các vấn đề điều khiển bám đuổi tuần hoàn cho các tay máy công nghiệp. Bộ điều khiển này bao gồm hai vòng điều khiển. Ở vòng điều khiển bên trong, một tín hiệu điều khiển vi-phân-tỉ-lệ đơn giản được sử dụng để ổn định hệ thống vòng kín, tạo điều kiện thuận lợi cho việc thiết kế các tín hiệu điều khiển ở vòng ngoài. Nhiệm vụ điều khiển chủ yếu được thực thi nhờ một tín hiệu điều khiển học lặp mới được thiết kế ở vòng ngoài. Tính hiệu quả của phương pháp điều khiển này đến từ một quan điểm mới về phương pháp xây dựng cấu trúc bộ điều khiển lặp, ở đó tín hiệu điều khiển trên trục lặp được tổng hợp một cách linh hoạt từ thông tin hiện tại và thông tin quá khứ của hệ thống. Cụ thể, một mạng thần kinh nhân tạo có cấu trúc phù hợp được phát triển để ước lượng các nhiễu động trên trục lặp dựa vào các thông tin tổng hợp vừa phân tích. Một hàm kế thừa mềm được sử dụng để kết nối tín hiệu điều khiển trên trục lặp và trục thời gian. Tính ổn định của quá trình học và cả hệ thống vòng kín được đảm bảo bằng tiêu chuẩn hồi quy nối tiếp. Tính hiệu quả và tính khả thi của bộ điều khiển đề xuất được thảo luận cẩn thận dựa trên các kết quả mô phỏng và thực nghiệm có tính so sánh từ một mô hình tay máy công nghiệp 6 bậc tự do.

1. Introduction

Nowadays, humans are passing through the fourth Industrial Revolution, in which robots play a key role both in industrial manufacturing and day-life activities. Proportional-Integral-Derivative (PID) controllers have been favorited in most industrial robots owing to their simplicity in implementation and acceptable control performances [1], [2]. High-accuracy controllers with great adaptation ability are required for

Received: 09 July 2022; Accepted: 07 August 2022.

modern robotic systems [3], [4]. However, unknown dynamical behaviors and complicated working environments are main obstacles on approaching excellent control outcomes [5]–[8]. To cope with unexpected effects of systematic dynamical models, many model-based controllers have been studied based on typical physical analyses such as force/torque-based or energy-based methods, or decomposition principles [9], [10]. In reality, applicability of such approaches would be limited with general robots and be more difficult for higher degree-of-freedom robots. Owing to universal approximation properties, neural-network-based control approaches have been recently increasingly employed in robotic systems [11]–[13]. Direct and indirect learning methods are the leading solutions for building neural networks [7], [14]. The system dynamics could be estimated by neural-networks and their results could be then adopted to eliminate unknown effects in control processes. This kind of the design has been successfully utilized by the many types of the networks such as Radial-basis function (RBF) networks [11], [15], [16] or Fuzzy-hybrid networks [17], [18]. Excellent control performances have been exhibited by such the intelligent controllers. For repetitive control missions that commonly occurs in industrial activities, the neural-network-based control approaches need to be modified for outstanding control outcomes.

Iterative learning control (ILC) technique is a famous control framework for systems with repetitive tasks. Its key idea is to iteratively compute a control input based on errors from previous trails so that the performance of the system can be optimized. Previous work [19], [20] shows that with simple designs, the ILC methods could provide superior performances by effectively tackling repetitive disturbances such as gravity and model uncertainties. In fact, the disturbances and nonlinear uncertainties are rarely repetitive terms. In most robotic systems, both iteration-varying and iteration-invariant disturbances exist on the iterative direction. Iteration-varying disturbances can be divided into two types: Type I – state independent disturbances, for example external disturbances, and Type II - internal state-dependent disturbances, for example friction forces. To extensively tackle Type-I iterative disturbances, many advanced ILC approaches have been studied. ILC methods with robust learning filters, such as frequency or time-frequency filters, were used to isolate iteration-varying disturbances from out of the iterative loop. Indeed, in [21], low-pass filters were employed to separate model uncertainties at high frequencies, or in [22], a notch Q filter and a disturbance observer were injected to the ILC to handle external vibration disturbances concentrated at certain frequencies. In [23], a time-frequency numerical Q filter was proposed based on robust principal component analysis (RPCA) to eliminate the non-repetitive disturbances. In [24], another robust Q-filter-based ILC method was studied incorporated with a tuned feedback control signal to deal with both repetitive and non-repetitive perturbances. As comparing to Type-I ones, Type-II disturbances always varies on the iterative axis due to the dependence on system states. To treat the non-repetitive disturbances, a former adaptive ILC (AILC) method was proposed by Kuc and Lee [25] based on Lyapunov theories. The key idea of AILC for robotic systems, as discussed in [26], [27], is to adopt an adaptive signal which iteratively recognizes and compensates for unknown disturbances and uncertainties in the system dynamics. Generally, the algorithm requires an assumption that parameters of the robotic model are constants within one iteration [28], [29]. Recently, the ILC scheme was also integrated into a time-based adaptive control signal to yield promising control outcomes [30]. From the above analyses, since the iterative disturbances are state-, time- and iterative-dependent factors, using iterative control signals that are completely constructed from previous iteration information is difficult to yield outstanding control performances.

To fill in this gap with a simple-yet-universal control method, in this paper, we propose a PD neural-network-based iterative learning controller for position-tracking control of robotic manipulators. The control scheme has two loops: time-based loop and iterative-based loop. On the time direction, a PD control signal is used to bring the system states to the desired state as closely as possible. The control performance is then significantly improved along the iterative axis. Contributions of the paper are listed as follows:

1) A neural network with a nonlinear learning procedure is built up on the iterative axis to effectively tackle both the time- and iterative-based disturbances.
2) A new iterative control law is designed based on a flexible inherent function and the neural network designed to realize the control mission.
3) Stability of the closed-loop system is rigorously proven by regression series criteria.
4) Effectiveness and feasibility of the proposed ILC controller are carefully verified by intensive simulation and real-time experiments on a 6DOF robot model.

The remaining of the paper is structured as follows. Dynamics of general robotic manipulators are briefly reviewed, and control objectives are then stated in Section 2. Design of the proposed controller including a proportional-derivative control term, adaptive iterative learning control signal and stability analyses of the overall system are clearly presented in Section 3. Effectiveness and feasibility of the proposed control system are discussed in Section IV. Conclusions are finally drawn in the last section.

2. System Modeling and Problem Statements

Motion equations of a serial *n*-DOF robot is generally formulated using the following dynamics [6], [10], [31]:

$$\mathbf{M}\lfloor \mathbf{q} \rfloor \ddot{\mathbf{q}} = -\mathbf{C}\lfloor \mathbf{q}, \dot{\mathbf{q}} \rfloor \dot{\mathbf{q}} - \mathbf{g}\lfloor \mathbf{q} \rfloor + \mathbf{f}\lfloor \dot{\mathbf{q}} \rfloor + \boldsymbol{\tau}_{\mathbf{d}} + \boldsymbol{\tau} \quad (1)$$

where $\mathbf{q}, \dot{\mathbf{q}}, \boldsymbol{\tau} \in \Re^n$ denote the joint position, angular velocities, and the control torques, respectively, $\mathbf{M} \in \Re^{n \times n}$ is the inertia-mass matrix, $\mathbf{C}\dot{\mathbf{q}}, \mathbf{g}, \mathbf{f}, \boldsymbol{\tau}_{\mathbf{d}} \in \Re^n$ denote the Coriolis/Centripetal effect, the gravitational torque, frictional torque, and external disturbances, respectively.

Assumption 1: The unknown disturbance $(\boldsymbol{\tau}_d)$ is bounded [8], [11], [30].

Remark 1: We assume that the system states $(\mathbf{q}, \dot{\mathbf{q}})$ are measurable. We define a tracking control error synthesized from a desired profile $(\mathbf{q}_{\mathbf{d}})$ that is assumed to be a known, bounded and twice continuously differentiable signal, and the system output $(\mathbf{q})$. The main objective here is to develop a model-free intelligent ILC for high control accuracy of the robotic system (1). Unknown internal dynamics and complicated external disturbances from various working conditions are major barriers challenging the expected control performance. However, one important advantage of the control system is that it can run in many iterations. Other required features of the ongoing controller are model-free, adaptive and robust.

3. Flexible Neural Iterative Learning Controller

This section presents a detailed procedure of designing the proposed controller which consists of a simple PD-type control signal and an advanced iterative learning control term. Proper theoretical proofs are associated to the respective sections to explain effectiveness of the developed features.
The main control objective is defined as the following error

$$\mathbf{e} = \mathbf{q} - \mathbf{q_d} \tag{2}$$

To complete the tracking control mission, the final control signal is simply designed as follows:

$$\boldsymbol{\tau} = \boldsymbol{\tau}_t + \boldsymbol{\tau}_i \tag{3}$$

where τ_t and τ_i are time-based and iterative-base control terms.

3.1. Time-based PD Control signal

For high-precision control of the manipulators, one could use various types of the linear or nonlinear control methods [1], [32], [33]. Purpose of the time-domain control signal τ_t is however to stabilize the closed-loop system and bring the system output to the desired profile as closely as possible. In this approach, we only structure the control signal by a simplest control form with the following PD design:

$$\boldsymbol{\tau}_t = -\mathbf{K}_{Pt}\mathbf{e} - \mathbf{K}_{Dt}\dot{\mathbf{e}} \tag{4}$$

where $\mathbf{K}_{Pt}$ and $\mathbf{K}_{Dt}$ are diagonal positive-definite gain matrices.
By using the time-based PD control law (6), the closed-loop system is bounded stable with any positive control gains $\boldsymbol{K}_{Dt}$ and $\boldsymbol{K}_{Pt}$. However, the control accuracy needs to be further investigated. Here, we define the following indirect control objective [11], [34]:

$$\boldsymbol{\varepsilon} = \dot{\mathbf{e}} + \mathbf{K}_i\mathbf{e} \tag{5}$$

where $\mathbf{K}_i = \mathbf{K}_{Dt}^{-1}\mathbf{K}_{Pt}$ is the positive control gain matrix. In previous work, the new control objective is normally called as sliding-mode manifold [15], [44], [45].
The dynamics (1) could be re-expressed in terms of the new composited variable (17) in a scope of iterative axis:

$$\mathbf{M}_i\dot{\boldsymbol{\varepsilon}}_i = -\mathbf{C}_i\boldsymbol{\varepsilon}_i + \boldsymbol{\tau} - \mathbf{d}_i \tag{6}$$

where $\mathbf{d}_i$ is the lumped disturbance of the system in the iteration *i*, that includes the model deviation and external disturbance:

$$\mathbf{d}_i = \mathbf{M}_i\left(\ddot{\mathbf{q}}_d - \mathbf{K}_i\dot{\mathbf{e}}_i\right) + \mathbf{C}_i\left(\dot{\mathbf{q}}_d - \mathbf{K}_i\mathbf{e}_i\right) + \mathbf{g}_i - \mathbf{f}_i - \boldsymbol{\tau}_{\mathbf{d}i} \tag{7}$$

Note that under the virtue of the control rule (4)-(5), such the disturbance $\mathbf{d}_i$ is bounded. The steady-state control error of the system will approach to the following range [25][30]:

$$\mathbf{e}_{ss} = \lim_{t\to\infty}\left(\mathbf{K}_{Pt}^{-1}\left(\mathbf{d}_i - \boldsymbol{\tau}_i\right)\right) \tag{8}$$

Remark 2: The control error could be reduced by selecting large control gains $\boldsymbol{K}_{Dt}$ and $\boldsymbol{K}_{Pt}$. However, to achieve excellent control performance, the nonlinear uncertainties and disturbances in the system dynamics must be compensated. To this end, possible directions are adoption of robust adaptive nonlinear controllers [8], [36] or high-gain observers [14], [37]. In fact, the dynamical behaviors of the system would be stored in the previous iteration data. Properly exploiting such the data could lead to interesting control outcomes.

3.2. Neural Iterative-based Control Signal

By utilizing from the advantages of the iterative control technique and repetitive control behaviors, in this subsection, an advanced iterative-based control signal is designed to provide good tracking control error of the closed-loop system.
Inspired but different from previous work [32], [48], [49], the iterative control law is selected as

$$\boldsymbol{\tau}_i = \mathbf{B}_i\boldsymbol{\tau}_{i-1} + \boldsymbol{\xi}_i \tag{9}$$

where $\mathbf{B}_i = \text{diag}\lfloor \mathbf{b}_i \rfloor$ is a diagonal matrix of inheritance function and $\boldsymbol{\xi}_i$ is the excitation function.

Also from the work, the iterative disturbance $\mathbf{d}_i$ was assumed to be no change on the iterative direction, and such the excitation function was simply selected as

$$\boldsymbol{\xi}_i = \boldsymbol{\varepsilon}_{i-1} \tag{10}$$

As carefully observing in the form of (7), the assumption on invariant properties of the disturbance $\mathbf{d}_i$ is weak. With such the design, the iterative control signal has tended to completely believe the past results. Much research in human society show that this action is not an appropriate choice [38], [39]. Hence, in this paper, another point of view in this design is required to deal with the aforeanalyzed problem. The constraint (8) implies that once the iterative control signal $\boldsymbol{\tau}_i$ approaches to the disturbance $\mathbf{d}_i$, the control error would converge to zero or as small as possible. It is worth defining a new error:

$$\boldsymbol{\varsigma}_i = \boldsymbol{\tau}_i - \mathbf{d}_i \tag{11}$$

By noting the general control rule (9), variation of the new error on the iteration axis is

$$\boldsymbol{\varsigma}_i = \mathbf{B}_i\boldsymbol{\varsigma}_{i-1} + \boldsymbol{\xi}_i - \boldsymbol{\varphi}_{i,i-1} \tag{12}$$

where $\boldsymbol{\varphi}_{i,i-1}$ is called as the iterative disturbance:

$$\boldsymbol{\varphi}_{i,i-1} = \mathbf{d}_i - \mathbf{B}_i\mathbf{d}_{i-1} \tag{13}$$

The new disturbance $\boldsymbol{\varphi}_{i,i-1}$ depends both on the current and past states on both time and iterative axes. It can be seen that once $\mathbf{e}_i$ approaches to $\mathbf{e}_{i-1}$, the disturbance $\mathbf{d}_i$ will approach to $\mathbf{d}_{i-1}$. Based on this observation, the inheritance function could be selected as

$$b_{i,k|k=1..n} = \tanh(\sigma_{1,k}t)\left(1 - \tanh(\sigma_{2,k}\varepsilon_{i,k}^2)\right) \tag{14}$$

where $\sigma_{1,k}$ and $\sigma_{2,k}$ are positive constants.

To design the excitation function, we start with approximating the new disturbance $\boldsymbol{\varphi}_{i,i-1}$ using universal approximation properties of neural networks [4], [40], as follows:

$$\varphi_{i,i-1,k|k=1..n} = \mathbf{w}_{i,k}^T \mathbf{r}_i \lfloor \mathbf{q}_i, \dot{\mathbf{q}}_i, \mathbf{q}_{i-1}, \dot{\mathbf{q}}_{i-1}, \mathbf{q}_d, \dot{\mathbf{q}}_d \rfloor + \varpi_{i,k} \quad (15)$$

where $\mathbf{w}_{i,k}$ is the optimal weight matrix, $\mathbf{r}_i$ is a regression vector, and $\varpi_{i,k}$ is the approximation error. Here the regression vector $\mathbf{r}_i$ is structured by 1-norm elements or $0 \le r_{i,j|j=1...m} \le 1$, in which m is the length of the vector.

Role of the excitation function $\boldsymbol{\xi}_i$ is to eliminate the new disturbance $\boldsymbol{\varphi}_{i,i-1}$, it is hence designed as

$$\xi_{i,k|k=1..n} = \hat{\mathbf{w}}_{i,k}^T \mathbf{r}_i \lfloor \mathbf{q}_i, \dot{\mathbf{q}}_i, \mathbf{q}_{i-1}, \dot{\mathbf{q}}_{i-1}, \mathbf{q}_d, \dot{\mathbf{q}}_d \rfloor \quad (16)$$

where $\hat{\mathbf{w}}_{i,k}$ is estimate of the $\mathbf{w}_{i,k}$.

By substituting the selection (16) to the variation (12), we have

$$\varsigma_{i,k|k=1..n} = b_i \varsigma_{i-1,k} + \tilde{\mathbf{w}}_{i,k}^T \mathbf{r}_i - \varpi_{i,k} \quad (17)$$

where $\tilde{\mathbf{w}}_{i,k} = \hat{\mathbf{w}}_{i,k} - \mathbf{w}_{i,k}$ is estimation error.

It can be observed that the iterative control performance completely depends on the learning of the excitation function. Hence, we select the following learning law:

$$\hat{\mathbf{w}}_{i,k|k=1..n} = \left(\mathbf{I} - \gamma_{i,w,k} \mathrm{diag}\lfloor \mathbf{r}_i \rfloor\right) \hat{\mathbf{w}}_{i-1,k} - \beta_{i,k} \frac{\mathbf{r}_i \tanh\lfloor \varepsilon_{i,k} \rfloor}{1 + \mathbf{r}_i^T \mathbf{r}_i} \quad (18)$$

where $0 < |\gamma_{i,w,k}| < 1, 0 < \beta_{i,k}$ are constants, and $\boldsymbol{I}$ is the relative identity matrix.

Effectiveness of the flexible iterative control mechanism is investigated from the following statement.

Theorem 1: For any bounded iterative disturbance that is expressed in a linear combination as presented in (15), if employing the iterative control signal (9), (14) and the nonlinear learning rule (18), the following properties hold:

1) The estimation error $\tilde{\mathbf{w}}_{i,k}$ will be stabilized inside an arbitrary small vicinity around zero.

2) The iterative control signal $\boldsymbol{\tau}_i$ is bounded.

Proof:

From the learning law (18), variation of the estimation error on the iterative direction is

$$\tilde{\mathbf{w}}_{i,k|k=1..n} = \left(\mathbf{I} - \gamma_{i,w,k} \mathrm{diag}[\mathbf{r}_i]\right) \tilde{\mathbf{w}}_{i-1,k} - \mathbf{w}_{i,k} + \left(\mathbf{I} - \gamma_{i,w,k} \mathrm{diag}[\mathbf{r}_i]\right) \mathbf{w}_{i-1,k} - \beta_{i,k} \frac{\mathbf{r}_i \tanh\lfloor \varepsilon_{i,k} \rfloor}{1 + \mathbf{r}_i^T \mathbf{r}_i} \quad (19)$$

By applying triangle inequality to (19), we get the following regression constraint:

$$\begin{aligned} \|\tilde{\mathbf{w}}_{i,k|k=1..n}\| &\le \bar{\lambda}_{(\mathbf{I}-\gamma_{i,w,k}\mathrm{diag}[\mathbf{r}_i])} \|\tilde{\mathbf{w}}_{i-1,k}\| \\ &+ \left(1 + \bar{\lambda}_{(\mathbf{I}-\gamma_{i,w,k}\mathrm{diag}[\mathbf{r}_i])}\right) \|\bar{\mathbf{w}}_{i,k}\| + \beta_{i,k} \le ... \le \bar{\lambda}^i_{(\mathbf{I}-\gamma_{i,w,k}\mathrm{diag}[\mathbf{r}_i])} \|\tilde{\mathbf{w}}_{0,k}\| \\ &+ \frac{1 - \bar{\lambda}^{i-1}_{(\mathbf{I}-\gamma_{i,w,k}\mathrm{diag}[\mathbf{r}_i])}}{1 - \bar{\lambda}_{(\mathbf{I}-\gamma_{i,w,k}\mathrm{diag}[\mathbf{r}_i])}} \left(\left(1 + \bar{\lambda}_{(\mathbf{I}-\gamma_{i,w,k}\mathrm{diag}[\mathbf{r}_i])}\right) \|\bar{\mathbf{w}}_{i,k}\| + \beta_{i,k} \right) \end{aligned} \quad (20)$$

where $\bar{\lambda}_{(\mathbf{I}-\gamma_{i,w,k}\mathrm{diag}[\mathbf{r}_i])} = \max\lfloor \mathrm{eig}\lfloor \mathbf{I} - \gamma_{i,w,k} \mathrm{diag}[\mathbf{r}_i] \rfloor \rfloor$ is the maximum eigen value of the matrix $(\mathbf{I} - \gamma_{i,w,k} \mathrm{diag}[\mathbf{r}_i])$, and $\bar{\mathbf{w}}_{i,k} = \max\lfloor |\mathbf{w}_{i,k}| \rfloor$ is the upper bound of the weight vector $(\mathbf{w}_{i,k})$.

For deactivation cases where the regression-vector elements are equal zero or $(r_{i,j|j=1...m} = 0)$, according to (18), the estimation weight vector $(\hat{\mathbf{w}}_{i,k})$ is boundedly preserved through iterative to iterative.

For activation cases where the regression-vector elements have the values of $(0 < r_{i,j|j=1...m} \le 1)$, the regression ratio is inside the unit circle or $0 < \bar{\lambda}_{(\mathbf{I}-\gamma_{i,w,k}\mathrm{diag}[\mathbf{r}_i])} < 1$. Furthermore, the ideal weight vector $(\mathbf{w}_{i,k})$ is bounded. If the initial value $(\hat{\mathbf{w}}_{0,k})$ is boundedly selected, from (20), the estimation error vector $(\tilde{\mathbf{w}}_{i,k})$ is bounded. The first statement of Theorem 1 is thus proven. □

By noting (16) and (18), the variation (9) could be rewritten as

$$\tau_{i,k|k=1..n} = b_i \tau_{i-1,k|k=1..n} + \mathbf{r}_i^T \left(\mathbf{I} - \gamma_{i,w,k} \mathrm{diag}[\mathbf{r}_i]\right) \hat{\mathbf{w}}_{i-1,k} - \beta_{i,k} \frac{\mathbf{r}_i^T \mathbf{r}_i \tanh\lfloor \varepsilon_{i,k} \rfloor}{1 + \mathbf{r}_i^T \mathbf{r}_i} \quad (21)$$

Taking absolute values at both sides of (21) in the regression manner results in the following inequality:

$$\begin{aligned} |\tau_{i,k|k=1..n}| &\le \bar{b} |\tau_{i-1,k|k=1..n}| \\ &+ \bar{\lambda}_{(\mathbf{I}-\gamma_{i,w,k}\mathrm{diag}[\mathbf{r}_i])} \|\bar{\hat{\mathbf{w}}}_{i-1,k}\| \|\mathbf{r}_i\| + \alpha\beta_k \le ... \le \bar{b}^i |\tau_{0,k|k=1..n}| \\ &+ \frac{1 - \bar{\lambda}^i_{(\mathbf{I}-\gamma_{i,w,k}\mathrm{diag}[\mathbf{r}_i])}}{1 - \bar{\lambda}_{(\mathbf{I}-\gamma_{i,w,k}\mathrm{diag}[\mathbf{r}_i])}} \|\bar{\hat{\mathbf{w}}}_{i-1,k}\| \|\mathbf{r}_i\| + \frac{1 - \alpha^i}{1 - \alpha} \beta_k \end{aligned} \quad (22)$$

where $\bar{b} = \max\lfloor b_{i,k|k=1..n} \rfloor$ is the maximum value of the inheritance function (b_i), $\bar{\hat{\mathbf{w}}}_{i-1,k} = \max\lfloor |\hat{\mathbf{w}}_{i-1,k}| \rfloor$ is the upper bound of the estimation weight vector $(\hat{\mathbf{w}}_{i,k})$, $\tau_{0,k|k=1..n}$ is the initial iterative control torque, and α is a constant that is defined as:

$$0 \le \alpha = \max\left\lfloor \frac{\mathbf{r}_i^T \mathbf{r}_i}{1 + \mathbf{r}_i^T \mathbf{r}_i} \right\rfloor < 1 \quad (23)$$

By using the result of the first statement in which the upper bound $\bar{\hat{\mathbf{w}}}_{i-,k}$ is bounded. From (14), the inheritance gain $(\bar{b})$ is inside the unit circle or $(0 \le \bar{b} < 1)$. From (22), the iterative control torque $\tau_{i,k|k=1..n}$ is thus bounded under the constraint (23). □

Remark 3: With properly selecting the regression vector $\mathbf{r}_i$, the approximation error $\varpi_{i,k}$ could be minimized. As a sequence, according to the dynamics (17), the iterative control error (11) would be minimized as well thanks to the results of *Theorem 1*. Note that the approximation effect of the neural-network model (15) comes from the structure of the regression vector $\mathbf{r}_i$ [4], [40]. It is recommended that the vector $\mathbf{r}_i\lfloor \mathbf{q}_i,\dot{\mathbf{q}}_i,\mathbf{q}_{i-1},\dot{\mathbf{q}}_{i-1},\mathbf{q}_d,\dot{\mathbf{q}}_d \rfloor$ is designed to normally reflect information of the inputs $(\mathbf{q}_i,\dot{\mathbf{q}}_i,\mathbf{q}_{i-1},\dot{\mathbf{q}}_{i-1},\mathbf{q}_d,\dot{\mathbf{q}}_d)$ over their workspaces. In the proposed control algorithm, the regression vector $\mathbf{r}_i$ has to belong to the 1-norm class. It could be encoded by *radial-basis* functions, or *logsig* function, or *tansig* functions, etc.

Remark 4: In fact, to obtain excellent control error (5), one could employ neural networks to learn the disturbance (7) using current states of the system (1). As presented in (15), the regression vector of the iterative-based neural network contains more state than that of the time-based networks. Hence, by using the iterative control technique, one could utilize the control experiences in the past to result in higher control performances. Indeed, the control accuracy is improved along the variation (9) once the network well estimates the iterative behaviors.

Remark 5: The proposed control idea is graphically summarized in **Fig. 1**. The algorithm can be implemented by the following procedure. In *the first step*, the iterative-based control signal is turned off, and the time-based control signal is employed to stabilize the main control objective (2) with proper control gains $(\mathbf{K}_{\mathbf{Dt}},\mathbf{K}_{\mathbf{Pt}})$. In *the second step*, the iterative control signal (9) is activated, but the inheritance function $(\mathbf{b}_i)$ is set to be zero. The regression vector $\mathbf{r}_i\lfloor \mathbf{q}_i,\dot{\mathbf{q}}_i,\mathbf{q}_{i-1},\dot{\mathbf{q}}_{i-1},\mathbf{q}_d,\dot{\mathbf{q}}_d \rfloor$ is next designed based on the workspace of its inputs, which have been observed from the previous step. The neural weight vector ($\hat{\mathbf{w}}_{i,k}$) is then updated by the learning rule (18) with proper learning gains $0<\left|\gamma_{i,w,k}\right|<1, 0<\beta_{i,k}$. In *the third step*, the inheritance function $(\mathbf{b}_i)$ is turned on with appropriate positive constants $\sigma_{1,k}$ and $\sigma_{2,k}$ using the constraint (14). One could be back to *Step 1* or *Step 2* for fine tuning the gains in several times until the expected control performance is resulted in.

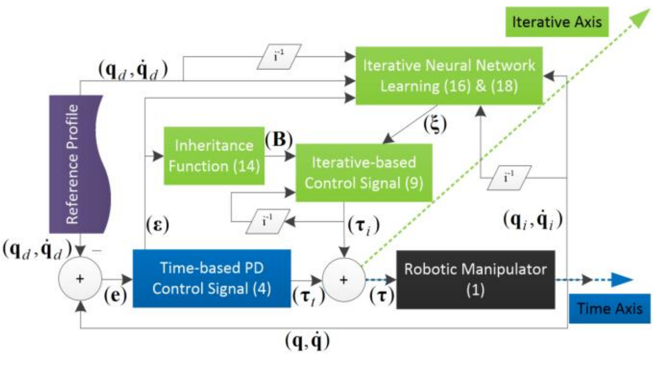

Figure 1: Block diagram of the proposed controller.

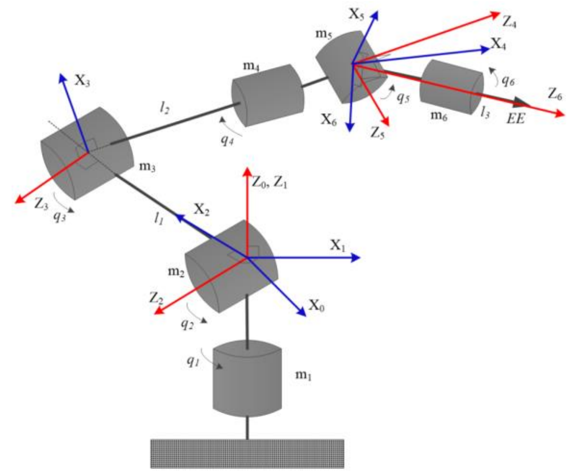

Figure 2: Configuration of the simulation robot.

4. Validation Results

The control performance of the proposed controller (**PDINN**) was carefully verified both in simulation and real-time experiments. To clearly evaluate the advantages of the proposed ILC method, a conventional proportional-derivative (**PD**) controller [1], time-based neural-network (**TNN**) controller [42], and conventional adaptive iterative learning controller (**TNNIC**) [30] were implemented to control the same system under same working conditions.

4.1. Simulation Results

The controllers were first tested on a 6-Degree-of-freedom (6DOF) robot, as sketched in **Fig. 2**. Its dynamics could be referred from previous work [10], [42]. Parameters of the robotic model were selected as:

$$\begin{cases} l_1 = 0.2(m); l_2 = 0.3(m); l_3 = 0.2(m); \\ m_1 = 2.2(kg); m_2 = 2.4(kg); m_3 = 2.05(kg); \\ m_4 = 0.32(kg); m_5 = 0.19(kg); m_6 = 0.18(kg); \end{cases}$$

In the simulation tests, the learning and control gains of the proposed controller were chosen as follows:

$$\begin{cases} \mathbf{K}_{Pt} = 150\mathbf{I}_6; \mathbf{K}_{Dt} = 10\mathbf{I}_6; \\ \boldsymbol{\sigma}_1 = 3\mathbf{I}_6; \boldsymbol{\sigma}_2 = 0.0048\mathbf{I}_6 \\ \gamma_{i,w,k|k=1..6} = 0.1; \boldsymbol{\beta}_1 = 12\mathbf{I}_6. \end{cases}$$

Hidden layers of the neural network had 1944 neurons that were encoded using *logsig* functions. The initial joint positions were set to be zero. The desired profiles of the robot joints were chosen with various types of the sinusoidal and smooth-multistep signals, as follows:

$$\begin{cases} q_{1d} = \sin(0.4\pi t); q_{2d} = \dfrac{2}{1+e^{-10t}} - \dfrac{2+e^{-20t+40}}{1+e^{-20t+40}}; \\ q_{3d} = 1.2\sin(\pi t); q_{4d} = 1.1\sin(1.5\pi t) \\ q_{5d} = \dfrac{1}{1+e^{-15t}} - \dfrac{1}{1+e^{30t-450}}; q_{6d} = 1.2\sin(2\pi t);. \end{cases}$$

In the first simulation, external disturbances that affect to the joint motions were also added to the system, as depicted in **Fig. 3**. These disturbances were no change on the iteration axis. Simulation results of the four controllers applied to the robot model in 10 iterations are shown in **Figs. 4 – 6**.

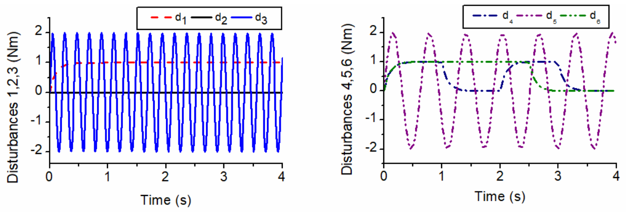

Figure 3: External disturbances affecting to the robot joints in the first simulation.

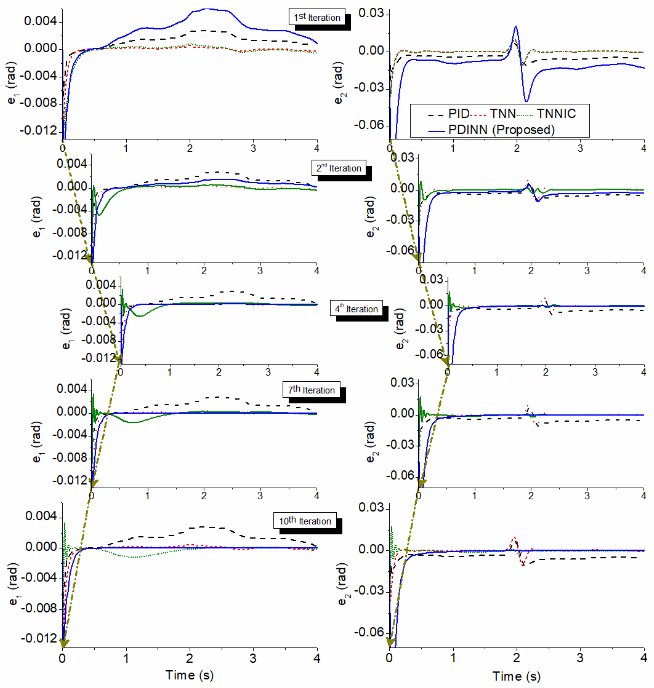

Figure 4: Comparative control errors of the controllers on the time axis and the iteration axis in the first simulation.

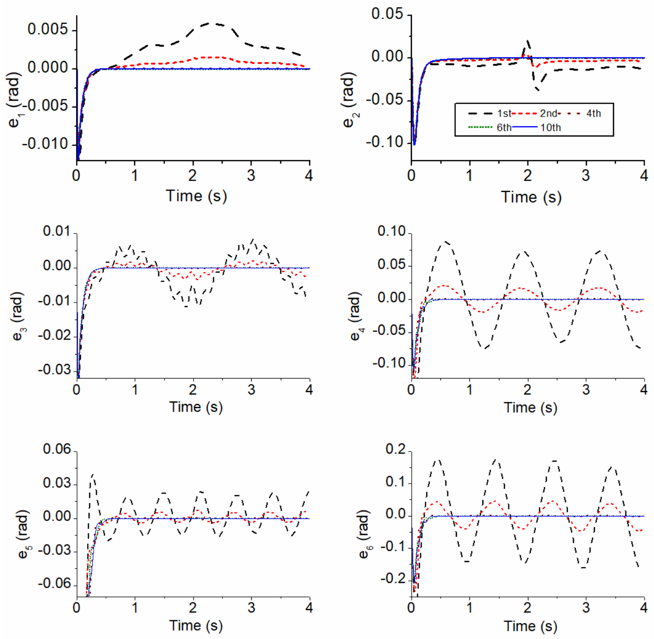

Figure 5: Control errors of the proposed controller on the time axis and the iteration axis in the first simulation.

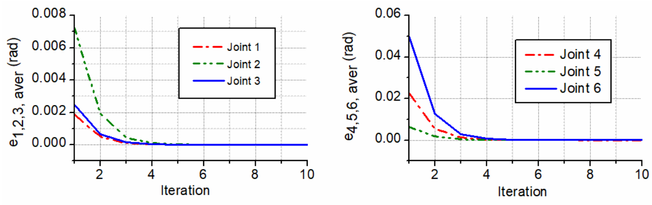

Figure 6: Average absolute control errors of the proposed controller on the iteration axis in the first simulation.

To make the report concise, only simulation results of joints 1 and 2 of the robot are presented in **Fig. 4**. As seen in this figure, even though working with the complicated robot, the PD controllers with well-tuned gains still obtained good control accuracies: 0.0028 (rad) and 0.011 (rad) respectively for joint 1 and 2 under harsh perturbances. The control performances could be improved by using learning properties of neural networks to approximate the nonlinear uncertainties and disturbances in the system dynamics on the time axis. Indeed, also as observed in **Fig. 4**, the neural controller always provided better control outcomes than the simple linear one. Control errors of the time-based neural network (TNN) controller were reduced to be: 0.0006 (rad) and 0.004 (rad) for the first and second joints, respectively. However, if the system worked in a repetitive manner, iterative-based control techniques could be applied and exhibited higher control performances. **Figure 4** shows that a combination of time-based neural-network control signal and a conventional iterative learning control term could suppress the disturbance more effectively and delivered promising control results: after 10 iterations, the control errors at the first and second joints were 0.00015 (rad) and 0.0006 (rad), respectively. However, high vibration phenomena could be observed from the conventional ILC data on the iterative axis. As an innovative step, in this paper, a new neural iterative control viewpoint is studied as clearly presented in Section 3. Its control effect is demonstrated by the control results shown in **Figs. 4, 5,** and **6**. In the first iteration, as depicted in **Fig. 4**, since the proposed control signal was just generated by a poor PD control framework and the ILC was not applied any more, its performances looked even worse than those of the well-tuned PD one. In the second iteration, at which the new ILC theory had been gone into operation, the control errors seemed to be enhanced in all the joints, but not better than those of other controllers, especially in joint 1 that was influenced by the severe external disturbances. However, a positive point could be observed here that is the system could be learnable. Interestingly, after 10 iterations, the proposed ILC approach could result in the best control performances under various working conditions: 0.000012 (rad) and 0.000054 (rad) for the first and second joints, respectively. The learning process of the new ILC technique is more clearly reflexed by the control errors summarized in **Figs. 5** and **6**. The data once again confirm that the proposed ILC scheme works well in various conditions even though it could start from a weak level.

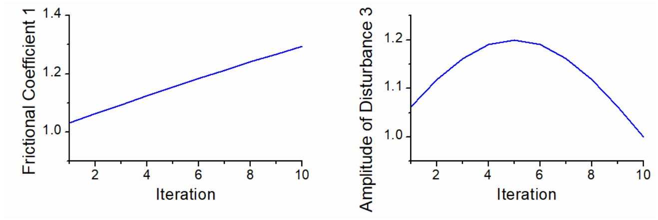

Figure 7: Variations of the frictional coefficient at joint 1 and the amplitude of external disturbances at joint 3 in the second simulation.

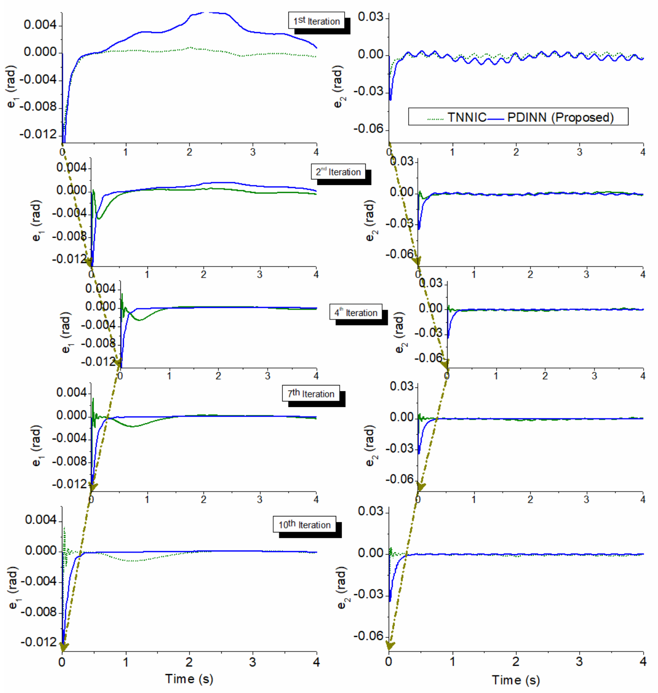

Figure 8: Comparative control errors of the iterative controllers on the time axis and the iteration axis in the second simulation.

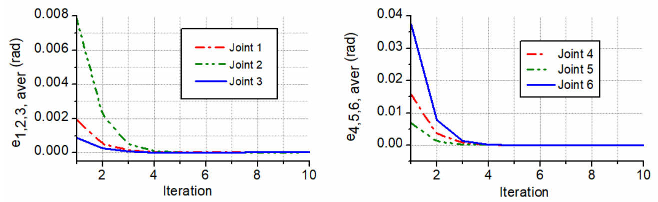

Figure 9: Average absolute control errors of the proposed controller on the iteration axis in the second simulation.

In the second simulation, to bring the developed algorithm close to practice, the controllers were challenged with non-repetitive external disturbance and internal parameter variations. The frictional coefficient at joint 1 and the amplitude of the external disturbance at joint 3 were set to be changed following the iterative schedules as presented in **Fig. 7**. In this test, only the iterative controllers (TNNIC and PDINN) were applied to control the system, and their working performances achieved are shown in **Figs. 8** and **9**. Figure 8 presents the control errors of the controllers at joints 1 and 3 of the robot. In the new testing conditions, that the disturbances changed in larger ranges obviously leads to degradation of the iterative control performances: for example, the steady-state control errors of the TNNIC controller at joints 1 and 3 increased to be 0.00035 and 0.00077, respectively. However, thanks to the strong support of the new iterative control theory proposed, as discussed in *Remark 3* as well as mathematical viewpoints in (14), (15), (17), (18) and *Theorem 1*, the designed controllers worked in a robust manner to result in good control outcomes: the new control accuracies at joints 1 and 3 were 0.000032 and 0.000045, respectively. As seen in **Fig. 9**, it can further confirm that the iterative controllers dealt with well both the repetitive and non-repetitive disturbances.

4.2. Experimental Results

Real-time experiments were conducted to investigate feasibility of the proposed controller. A 6DOF robot was designed and fabricated for the verification. The robot prototype is shown in **Fig. 10**. Industrial motors were used to drive the robot joints, and encoders with resolution of 5760ppr were adopted to measure the joint positions. A compact RIO 9024 controller connecting with digital (NI 9401) and analog (NI 9263) modules was employed as a data acquisition (DAQ) system. The algorithms were implemented in the Labview environment to control the second joint of the robot.

Figure 10: The experimental 6DOF robot.

The desired trajectory was chosen to be $q_{2d} = 1.4\left(\frac{2}{1+e^{-10t}} - \frac{2+e^{-20t+40}}{1+e^{-20t+40}}\right)$. The real-time control results achieved are presented in **Figs. 11** – **13**.

In the real-time experiments, as seen in **Fig. 11**, the time-based controllers (PD and TNN) still maintained their robustness with good control errors: 0.038 (rad) for the PD one and 0.014 (rad) for the TNN one. The data in **Fig. 11** present the learning effectiveness of conventional ILC method: the control accuracy after 10 iterations had been increased to 0.005 (rad). Even though governed by a strong time-based neural network control signal, the real-time experimental results however reveal that the nonlinearities, uncertainties and disturbances were not completely terminated using the conventional ILC one. We believe that such the problems could be efficiently tackled by the proposed ILC technology owing to the proper neural-network-based design (12), (14), (16), and (18). As demonstrated in detail in **Fig. 11** or in the summarization mode in **Fig. 12**, the developed ILC performance had been gradually improved from iteration to iteration: after 10 iterations, the steady-state control error reached to a good value of 0.0018 (rad). Average absolute values of the control errors for iterations obtained by the conventional and proposed ILC controller in the experiments are further compared in **Fig. 13**. The proposed controller has shown outperformance as comparing to the previous one. The convergence of the proposed ILC method is clearly confirmed via the detailed and statical data.

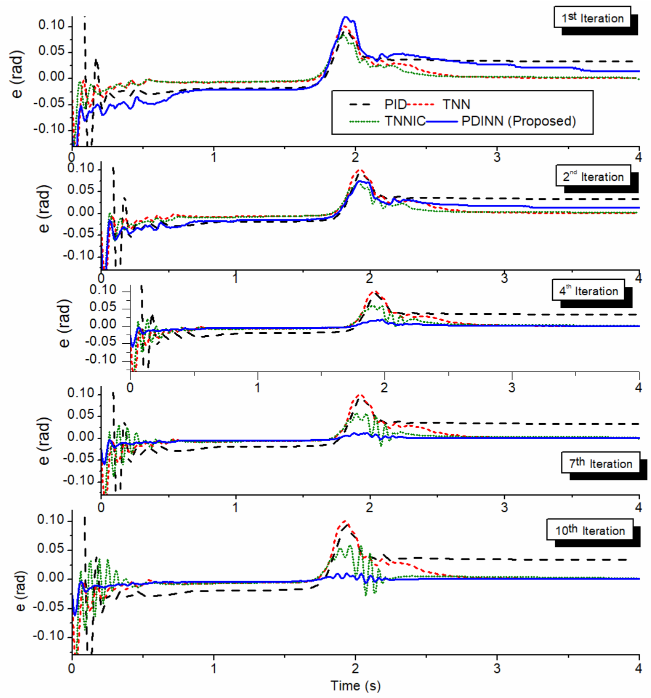

Figure 11: Comparative control errors of the controllers on time axis and iteration axis in the real-time experiments.

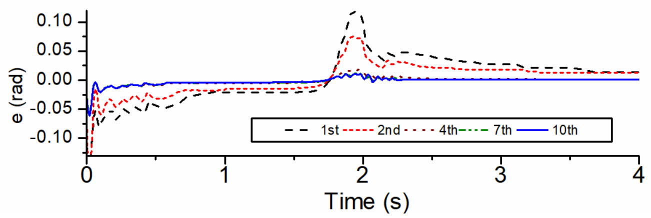

Figure 12: Control errors of the proposed controller on time axis and iteration axis in the real-time experiments.

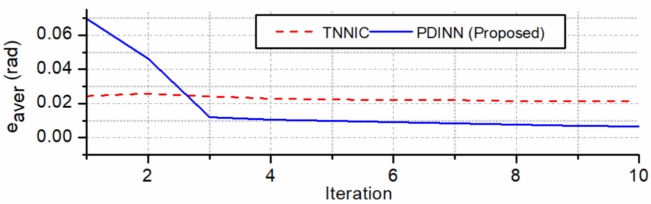

Figure 13: Average absolute control errors of the proposed controller on iteration axis in the real-time experiments.

5. Conclusion

A new adaptive iterative learning controller has been developed for motion control problems of robotic manipulators using neural networks. The system is first stabilized by an ordinary PD control signal on the time axis. The control performance is next effectively enhanced by using a novel ILC signal generated from a new adaptation design. The learning information are collected from both previous and present iterations and are then processed by a nonlinear neural network in a reliable manner. Stability, effectiveness, and feasibility of the overall system are rigorously proven by theoretical analyses under regression series criteria and comparative validation results on a 6DOF robot model.

Acknowledgement

This research is funded by Vietnam National Foundation for Science and Technology Development (NAFOSTED) under grant number 107.01-2020.10

References

[1] P. Rocco, "Stability of PID control for industrial robot arms," *IEEE Trans. Robot. Autom.*, vol. 12, no. 4, pp. 606–614, 1996.

[2] ABB Cooperation, "Industrial Robot Controllers," *ABB Value Provider Program*, 2022. https://new.abb.com/products/robotics/controllers.

[3] W. Sun, Y. Wu, and X. Lv, "Adaptive neural network control for full state constrained robotic manipulator with actuator saturation and time-varying delays," *IEEE Trans. Neural Networks Learn. Syst.*, 2021.

[4] Q. Guo, Y. Zhang, B. G. Celler, and S. W. Su, "Neural adaptive backstepping control of a robotic manipulator with prescribed performance constraint," *IEEE Trans. Neural Networks Learn. Syst.*, vol. 30, no. 12, pp. 3572–3583, 2019.

[5] Y. Park, I. Jo, J. Lee, and J. Bae, "A dual-cable hand exoskeleton system for virtual reality," *Mechatronics*, vol. 49, no. November 2017, pp. 177–186, 2018, doi: 10.1016/j.mechatronics.2017.12.008.

[6] M. Wang and A. Yang, "Dynamic learning from adaptive neural control of robot manipulators with prescribe performance," *IEEE Trans. Syst. Man, Cybern. Syst.*, vol. 47, no. 8, pp. 2244–2255, 2017.

[7] D. X. Ba, T. Q. Dinh, and K. K. Ahn, "An integrated intelligent nonlinear control method for pneumatic artificial muscle," *IEEE/ASME Trans. Mechatronics*, vol. 21, no. 4, pp. 1835–1845, 2016.

[8] W. He, Y. Chen, and Z. Yin, "Adaptive neural network control of an uncertain robot with full-state constraints," *IEEE Trans. Cybern.*, vol. 46, no. 3, pp. 620–629, 2016.

[9] W.-H. Zhu, *Virtual Decomposition Control: Toward hyper degrees of freedom robots*. Springer-Verlag Berlin Heidelberg, 2010.

[10] J. J. Craig, *Introduction to Robotics: Mechanics and Control*, 3rd ed. Pearson Prentice Hall, USA, 2005.

[11] D. X. Ba and J. Bae, "A precise neural-disturbance learning controller of constrained robotic manipulators," *IEEE Access*, vol. 9, pp. 50381–50390, 2021.

[12] M. Wang, Y. Zou, and C. Yang, "System transformation-based neural control for full-state-constrained pure-feedback systems via disturbance observer," *IEEE Trans. Cybern. (Early Access)*, pp. 1–11, 2020, doi: 10.1109/TCYB.2020.2988897.

[13] L. Wu, Q. Yan, and J. Cai, "Neural network-based adaptive learning control for robot manipulators with arbitrary initial errors," *IEEE Access*, vol. 7, pp. 180194–180204, 2019.

[14] W. He, Y. Sun, Z. Yan, C. Yang, Z. Li, and O. Kaynak, "Disturbance observer-based neural network control of cooperative multiple manipulators with input saturation," *IEEE Trans. Neural Networks Learn. Syst.*, vol. 31, no. 5, pp. 1735–1746, 2020.

[15] M. Chen and S. S. Ge, "Adaptive neural output feedback control of uncertain nonlinear systems with unknown hysteresis using disturbance

observer," *IEEE Trans. Ind. Electron.*, vol. 62, no. 12, pp. 7706–7716, 2015.
[16] M. Wang, Z. Wang, H. Dong, and Q.-L. Han, "A novel framework for backstepping-based control of discrete-time strict-feedback nonlinear systems with multiplicative noises," *IEEE Trans. Automat. Contr.*, vol. 66, no. 4, pp. 1484–1496, 2021, doi: 0.1109/TAC.2020.2995576.
[17] F. Chao, D. Zhou, C.-M. Lin, L. Yang, C. Zhou, and C. Shang, "Type-2 fuzzy hybrid controller network for robotic systems," *IEEE Trans. Cybern.*, vol. 50, no. 8, pp. 3778–3792, 2020.
[18] Z. Liu, G. Lai, Y. Zhang, and C. L. P. Chen, "Adaptive fuzzy tracking control of nonlinear time-delay systems with dead-zone output mechanism Based on a novel smooth model," *IEEE Trans. Fuzzy Syst.*, vol. 23, no. 6, pp. 1998–2011, 2015, doi: 10.1109/TFUZZ.2015.2396075.
[19] M. Takegaki and S. Arimoto, "A new feedback method for dynamic control of manipulators," *J. Dyn. Syst. Meas. Control*, vol. 103, no. 2, pp. 119–125, 1981.
[20] P. Bondi, G. Casalino, and L. Gambardella, "On the iterative learning control theory for robotic manipulators," *IEEE J. Robot. Autom.*, vol. 4, no. 1, pp. 14–22, 1988.
[21] D. A. Bristow, M. Tharayil, and A. G. Alleyne, "A survey of iterative learning control," *IEEE Control Syst. Mag.*, vol. 26, no. 3, pp. 96–114, 2006.
[22] L. Sun, X. Chen, and M. Tomizuka, "Selective iterative learning control with non-repetitive disturbance rejection," 2014.
[23] C. Y. Lin, L. Sun, and M. Tomizuka, "Robust principal component analysis for iterative learning control of precision motion systems with nonrepetitive disturbances," in *American Control Conference (ACC)*, 2015, pp. 2819–2824.
[24] C. Peng, L. Sun, and M. Tomizuka, "Constrained iterative learning control with pso-youla feedback tuning for building temperature control," *IFACPapersOnLine*, vol. 50, no. 1, pp. 3135–3141, 2017.
[25] T. Kuc and J. S. Lee, "An adaptive learning control of uncertain robotic systems," in *Proceedings of the 30th IEEE Conference on Decision and Control*, 1991, pp. 1206–1211.
[26] B. H. Park, T. Y. Kuc, and J. S. Lee, "Adaptive learning control of uncertain robotic systems," *Int. J. Control*, vol. 65, no. 5, pp. 725–744, 1996.
[27] A. Tayebi, "Adaptive iterative learning control for robot manipulators," *Automatica*, vol. 40, no. 7, pp. 1195–1203, 2004.
[28] C. T. Hsu, C. J. Chien, and C. Y. Yao, "A new algorithm of adaptive iterative learning control for uncertain robotic systems," in *2003 IEEE International Conference on Robotics and Automation*, 2003, pp. 4130–4135.
[29] S. Yang, X. Fan, and A. Luo, "Adaptive robust iterative learning control for uncertain robotic systems," in *Proceedings of the 4th World Congress on Intelligent Control and Automation*, 2002, pp. 964–968.
[30] R. Lee, L. Sun, Z. Wang, and M. Tomizuka, "Adaptive iterative learning control of robot manipulators for friction compensation," *IFAC Papers OnLine*, vol. 52, no. 15, pp. 175–180, 2019.
[31] W.-H. Zhu, *Virtual Decomposition Control: Toward hyper degrees of freedom robots*. Springer-Verlag Berlin Heidelberg, 2010.
[32] G. Chen, B. Jin, and Y. Chen, "Nonsingular fast terminal sliding mode posture control for six-legged walking robots with redundant actuation," *Mechatronics*, vol. 50, pp. 1-15, August 2016.
[33] L. Wang, T. Chai, and L. Zhai, "Neural-network-based terminal slidingmode control of robotic manipulators including actuator dynamics," *IEEE Trans. Ind. Electron.*, vol. 56, no. 9, pp. 3296–3304, 2009, doi:10.1109/TIE.2008.2011350.
[34] D. X. Ba and J. Bae, "A nonlinear sliding mode controller of serial robot manipulators with two-level gain-learning ability," *IEEE Access*, vol. 8, pp. 189224–189235, 2020.
[35] J. Zhang, X. Liu, Y. Xia, Z. Zuo, and Y. Wang, "Disturbance observer based integral sliding-mode control for systems with mismatched disturbances," *IEEE Trans. Ind. Electron.*, vol. 63, no. 11, pp. 7040–7048, 2016.
[36] M. Wang, Y. Zhang, and C. Wang, "Learning from neural control for nonaffine systems with full state constraints using command filtering," *Int. J. Control*, vol. 93, no. 10, pp. 2392–2406, 2020, doi:10.1080/00207179.2018.1558285.
[37] B. Xu, D. Wang, Y. Zhang, and Z. Shi, "DOB-based neural control of flexible hypersonic flight vehicle considering wind effects," *IEEE Trans. Ind. Electron.*, vol. 64, no. 11, pp. 8676–8685, 2017.
[38] J. Mezirow, *A Critical Theory of Adult Learning and Education*. 1981.
[39] B. E. Neubauer, C. T. Witkop, and L. Varpio, "How phenomenology can help us learn from the experiences of others," *Perspect. Med. Educ.*, vol. 8, no. 2, pp. 90–97, 2019.
[40] J. Park and I. W. Sandberg, "Universal approximation using radial-basis-function networks," *Neural Comput.*, vol. 3, no. 2, pp. 246–257, 1991.
[41] S. S. Ge, C. C. Hang, and T. Zhang, "Adaptive neural network control of nonlinear systems by state and output feedback," *IEEE Trans. Syst. Man, Cybern. Part B*, vol. 29, no. 6, pp. 818–828, 1999.
[42] F. L. Lewis, D. M. Dawson, and C. T. Abdallah, *Robot Manipulator Control: Theory and Practice*, 2nd ed. Marcel Dekker, USA, 2004.